


eGastroenterology Gasdermin D deletion prevents liver injury and exacerbates extrahepatic damage in a murine model of alcohol-induced ACLF

Martí Ortega-Ribera,¹ Yuan Zhuang,¹ Veronika Brezani,¹ Radhika S Joshi,¹ Zsuzsanna Zsengeller,² Prashanth Thevkar Nagesh,¹ Aditi Datta,¹ Gyongyi Szabo ^{1,3}

To cite: Ortega-Ribera M, Zhuang Y, Brezani V, *et al*. Gasdermin D deletion prevents liver injury and exacerbates extrahepatic damage in a murine model of alcohol-induced ACLF. *eGastroenterology* 2025;3:e100151. doi:10.1136/egastro-2024-100151

► Prepublication history and additional supplemental material for this paper are available online. To view these files, please visit the journal online (<https://doi.org/10.1136/egastro-2024-100151>).

Received 13 October 2024
Accepted 27 February 2025



- <https://doi.org/10.1136/egastro-2024-100101>
- <https://doi.org/10.1136/egastro-2023-100009>
- <https://doi.org/10.1136/egastro-2024-100104>
- <https://doi.org/10.1136/egastro-2024-100166>
- <https://doi.org/10.1136/egastro-2023-100036>



© Author(s) (or their employer(s)) 2025. Re-use permitted under CC BY-NC. No commercial re-use. See rights and permissions. Published by BMJ Group.

For numbered affiliations see end of article.

Correspondence to

Professor Gyongyi Szabo;
gszabo1@bidmc.harvard.edu

ABSTRACT

Background Gasdermin D (GSDM-D), a key executor of pyroptosis, is increased in various liver diseases and contributes to disease progression. Alcohol induces inflammasome activation and cell death, which are both linked to GSDM-D activation. However, its role in alcohol-induced acute-on-chronic liver failure (ACLF) remains unclear.

Methods ACLF was induced in GSDM-D-deficient or wild-type (WT) mice by 28-day bile duct ligation surgery plus a single 5 g/kg alcohol binge leading to acute decompensation. Nine hours after the alcohol binge, blood, liver, kidney and cerebellum specimens were collected for analysis.

Results Active GSDM-D was significantly increased in humans and mice ACLF livers compared with both healthy controls and cirrhotic livers. GSDM-D-deficient mice with ACLF showed decreased inflammation, neutrophil infiltration and fibrosis in the liver, together with a reduction in pyroptotic, apoptotic and necroptotic death, compared with WT ACLF mice. Notably, GSDM-D-deficient mice also showed decreased liver regeneration and hepatocyte function. This was associated with an increase in senescence and expression of stem-like/cholangiocyte markers in the liver. Interestingly, in the kidney, GSDM-D-deficient mice showed an increase in histopathological damage score, decreased function and increased expression of necroptosis-related genes. In the cerebellum, GSDM-D deficiency increased the expression of neuroinflammation markers, astrocyte activation and apoptosis-related genes.

Conclusion Our data indicate that GSDM-D deficiency has organ-specific effects in ACLF. While it reduces inflammation, neutrophil activation, cell death and fibrosis in the liver, GSDM-D deficiency impairs the synthetic function and increases senescence in hepatocytes. GSDM-D deficiency also increases kidney injury and neuroinflammation in ACLF.

INTRODUCTION

Cirrhosis complications account for approximately 800 000 hospitalisations annually in the USA, with a large proportion of patients requiring intensive care and organ support

WHAT IS ALREADY KNOWN ON THIS TOPIC

- ⇒ Increased levels of gasdermin D (GSDM-D), a pivotal mediator of pyroptosis, have been described in many liver diseases, including partial hepatectomy, metabolic dysfunction-associated steatohepatitis and alcoholic-associated hepatitis, among others.
- ⇒ To date, the implication and modulation of GSDM-D in the context of alcohol-induced acute-on-chronic liver failure (ACLF) have remained unexplored.

WHAT THIS STUDY ADDS

- ⇒ Our study demonstrates that active GSDM-D expression is increased in ACLF.
- ⇒ We also identified a potential dual effect of pyroptosis inhibition by using GSDM-D knockout mice in ACLF, with a protective effect on the liver and a detrimental effect on extrahepatic organs, including the kidney and brain.

HOW THIS STUDY MIGHT AFFECT RESEARCH, PRACTICE OR POLICY

- ⇒ The findings provide a foundation for future research aimed at improving the diagnosis and development of ACLF, especially when targeting pyroptosis.
- ⇒ Our study also highlights a potential need for organ-selective intervention targeting GSDM-D.

due to acute-on-chronic liver failure (ACLF).¹ ACLF frequently develops in individuals with advanced fibrosis or cirrhosis with or without decompensation and is defined by the presence of hepatic or at least one extrahepatic organ failure (neurological, renal, circulatory or respiratory systems) and high mortality rates.^{2,3} With organ transplantation being the only effective treatment for these patients, the number and severity of organ failures dictate disease prognosis and outcome.

The immune system plays a central role in orchestrating the ACLF pathophysiology and multiorgan involvement.^{4,5} ACLF is characterised by high-grade systemic inflammation and

immune cell paralysis, leading to the overproduction of pro-inflammatory molecules, as well as excessive immune cell activation and recruitment of neutrophils to the site of injury, leading to cell death, tissue damage and organ failure.⁵ Different preclinical models of ACLF have identified the activation of distinct types of cell death during ACLF, including apoptosis, necroptosis and more recently pyroptosis.^{6,7} Nevertheless, the implication of pyroptosis in ACLF pathophysiology remains elusive.

Pyroptosis is a form of inflammatory cell death induced via inflammasome activation and caspase (CASP) 1-mediated proteolytic activation of gasdermin D (GSDM-D) and interleukin (IL)-1 β and IL-18.⁸ Cleaved GSDM-D subunits, also known as N-terminal GSDM-D (NT-GSDM-D), form pores in the plasma membrane that are required for IL-1 β /IL-18 release during pyroptotic cell death.⁹ Hepatocyte pyroptosis has been described to induce neutrophil extracellular traps (NETs) during hepatitis B virus-related ACLF, further exacerbating tissue damage, damage-associated molecular pattern (DAMP) release and disease perpetuation.¹⁰ On the other hand, cell-free NETs induced by alcohol or bile acids can directly promote pyroptotic cell death (IL-1 β release) in human hepatocytes *in vitro*,⁷ overall indicating a potential role of pyroptosis in hepatocyte fate during ACLF.

Given the increased GSDM-D expression in patients with ACLF and its key relevance in executing pyroptosis, in this manuscript, we explored the multiorgan implication of GSDM-D genetic deletion in a preclinical murine model of alcohol-induced ACLF.

MATERIALS AND METHODS

Animals

C57BL/6J mice were purchased from The Jackson Laboratory (Bar Harbor, Maine). GSDM-D-deficient KO in C57BL/6N background mice were generously provided by Dr Vishva Dixit (Genentech).¹¹ C57BL/6N WT mice were used as controls for GSDM-D KO experiments. The mice were housed in a specific pathogen-free mouse facility at Beth Israel Deaconess Medical Center (BIDMC), and all animal handling was performed in compliance with institutional guidelines, with ad libitum access to food and water and a light and dark cycle of 12L:12D. In the study, n refers to the number of animals. We selected a small sample size because deletion of GSDM-D in ACLF was evaluated *in vivo* for the first time in the present study, and therefore the initial intention was to gather basic evidence regarding its effect on ACLF pathophysiology. All animals were considered in this study.

BDL surgery

BDL surgery was performed as previously described¹² for 4 days in the morning. Due to the protective effect of liver X receptors on bile acid toxicity in females,¹³ only males were used for this study. Briefly, male WT or GSDM-D KO mice 10–14 weeks old were anaesthetised and placed on an operating pad. The mice were shaved and the skin

was disinfected with 70% ethanol. Through an abdominal incision, the common bile duct was identified and ligated. The abdomen and the peritoneum were closed with a running silk suture. For sham control mice, the same surgical procedure was performed without BDL. Animals were monitored during recovery and treated with buprenorphine (0.1 mg/kg) to avoid pain-induced stress after surgical intervention.

Alcohol binge administration

Acute administration of ethanol (5 g/kg) by oral gavage was adapted from Bertola *et al.*¹⁴ Briefly, a 47.3% (vol/vol) ethanol solution was prepared from pure alcohol (1000002000; Pharmco) in water. Volume administration to each mouse was calculated as follows: gavage volume (μ L) of 47.3% (vol/vol) solution for each mouse = mouse body weight (in grams) \times 15. The control group received water binge. Animals were randomised after BDL surgery based on cage number.

ACLF model

An alcohol-induced ACLF model was developed as previously shown in Ortega-Ribera *et al.*⁷ Briefly, advanced cholestatic liver fibrosis was induced by 28-day BDL surgery followed by a single alcohol binge to trigger acute liver damage. Animals were randomised after BDL surgery based on cage number. Due to overt behavioural movement activity and the sedative effect of alcohol, the experimenter could not be blinded to whether the animal was in the sham, BDL or ACLF group. Nine hours after the alcohol binge, the animals were euthanised for sample collection. The specimens were snap-frozen in liquid nitrogen and stored at -80°C for molecular analysis (cell death, inflammation, liver disease, kidney injury and neuroinflammation) or processed in 10% formalin for histology.

Human liver tissue

Human liver samples were obtained from the Liver Tissue Cell Distribution System, National Institutes of Health (Minneapolis, USA). Liver samples from patients with cirrhosis with primary biliary cholangitis with or without ACLF (n=5) were used for GSDM-D protein expression analysis, as shown in figure 1B. The demographic data of the patients can be found in online supplemental table 1. For human samples, n refers to the number of patients.

Enzyme-linked immunosorbent assay

Serum or tissue lysate levels of NE (DY4517), CXCL1 (DY453), IL-6 (DY406; R&D Systems), MCP1 (DY479; R&D Systems), IL-18 (DY7625; R&D Systems), KIM-1 (DY1817) and IL-1 β (MHSLB00) for mouse were quantified by using commercially available kits according to the manufacturer's instructions. All kits were purchased from R&D Systems.

Immunoblotting

Liver tissue was lysed in radioimmunoprecipitation (RIPA) buffer (BP-115-500; Boston BioProducts) containing

protease inhibitor cocktail (5872S; Cell Signaling Technology). Equal amounts of total protein lysates (20–50 µg) were run on 12.5% sodium dodecyl sulfate-polyacrylamide gel electrophoresis and transferred to a nitrocellulose membrane. Following blocking (5% bovine serum albumin (BSA) in Tris buffer containing 1% Triton X-100), blots were probed with primary and fluorescent secondary antibodies (IRDye 800 and 700 CW; LI-COR Biosciences). Blots were developed using the LI-COR reader for fluorescent signals. Data were represented as relative fluorescent units.

The following antibodies were used for WB analysis in mouse: CASP3 (9662; Cell Signaling Technology), CASP4 (42264; Cell Signaling Technology), CASP11 (ab180673; Abcam), GSDM-D (ab209845; Abcam) and CASP1 (AG-20B-0042-C100; AdipoGen); or human: GSDM-D (GTX116840; GeneTex). Glyceraldehyde-3-phosphate dehydrogenase (GAPDH, 60004-1; ProteinTech) was used as housekeeping control.

Biochemical assays

For liver injury, serum levels of bilirubin (MAK126; Sigma-Aldrich) and ALT (A525-240; Teco Diagnostics) were quantified following the manufacturer's instructions. To assess kidney function, we measured the levels of BUN (EIABUN; Thermo Scientific) in the serum.

Kidney histopathological analysis

Kidney histology was analysed by a renal expert using H&E staining on 5 µm paraffin-embedded sections. Each slide was carefully examined on tubular dilation (0–3 based on severity), cortical and medullary cast formation (0 for 'absent', 1 for 'minimal', 2 for 'some' and 3 for 'moderate'), neutrophil infiltrates (0 for 'absent' and 1 for 'present') and interstitial hypercellularity (0 for 'absent', 1 for 'minimal' and 2 for 'frequent'). The histopathological score was obtained by combining individual scores from the above-mentioned variables. Representative images were taken at 200× or 400× magnification on a bright-field microscope.

mRNA isolation and quantitative real-time PCR

Total RNA was extracted and purified with RNeasy Mini Kit (74106; Qiagen) according to the manufacturer's instructions. RNA concentration was quantified by a Nanodrop ND-1000 spectrophotometer (NanoDrop Technologies, Wilmington, Delaware, USA). A maximum amount of 1 µg RNA was reverse-transcribed using a High-Capacity cDNA Reverse Transcription Kit (1708891; Bio-Rad) in a cDNA Mastercycler X50s (Eppendorf), and qPCR was performed in a CFX96 Real-Time PCR System (Bio-Rad), using Sybr Green primers and PCR Master Mix (1725124; Applied Biosystems). RNA expression levels were normalised following the $2^{-\Delta\Delta Ct}$ method, with GAPDH as the housekeeping gene. Detailed primer sequences used in this study can be found in online supplemental table 2.

Flow cytometry

In Eppendorf tubes containing 0.5 M EDTA to prevent coagulation, 50 µL of peripheral blood was collected. Blood samples were incubated with a cocktail of antibodies (1:100 dilution) for 30 min on ice: APC/Cyanine7 Anti-Mouse CD45 Antibody (103116, clone 30-F11; Biolegend), Brilliant Violet 711 Anti-CD11b Rat Monoclonal Antibody (cat #101242, clone M1/70; Biolegend), Alexa Fluor 700 Anti-Ly-6C Rat Monoclonal Antibody (cat #128024, clone HK1.4; Biolegend) and Zombie NIR Fixable Viability Kit (cat# 423106; Biolegend). After 30 min, all samples were incubated with BD Phosflow Lyse/Fix Buffer (558049; BD Biosciences) following the manufacturer's protocol. Following Lyse/Fix, cells were washed twice with 1× phosphate-buffered saline (PBS) containing 2% fetal bovine serum (FBS) and resuspended in fluorescence-activated cell sorting (FACS) buffer containing 2% FBS in PBS. Samples were run in Aurora Spectral Flow Cytometer (Cytek) and data analysis was done using the FlowJo V.8.8.7 software.

Statistical analysis

Normality of the sample distribution was assessed using the Kolmogorov-Smirnov test. For samples fitting a normal distribution, the means were compared by Student's t-test (two groups) or analysis of variance (more than two groups), followed by the Tukey's post-hoc analysis. Otherwise, the means were compared using non-parametric Kruskal-Wallis test, followed by Mann-Whitney U test. Differences were considered significant at $p < 0.05$. Statistical analyses were performed using GraphPad Prism V.9 software for Windows (GraphPad Software, San Diego, California, USA).

RESULTS

NT-GSDM-D is increased in a preclinical model of ACLF and clinical liver specimens with ACLF

As the first step to decipher the role of GSDM-D in ACLF, we evaluated the protein expression of full-length (FL)-GSDM-D and N-terminal (NT)-GSDM-D in a preclinical model of alcohol-induced ACLF. GSDM-D expression in ACLF was compared with the expression of cirrhotic mice due to bile duct ligation (BDL) for 28 days or sham-operated healthy animals (figure 1A). Western blot analysis revealed a significant increase in both FL-GSDM-D and NT-GSDM-D expressions in the cirrhotic group compared with healthy mice (figure 1A). Moreover, fibrotic mice receiving a single alcohol binge (hereinafter referred to as ACLF mice) showed a further increase in active NT-GSDM-D expression (figure 1A). Next, we validated these findings in human liver samples from healthy individuals or patients with cirrhosis with or without ACLF. The demographic data of the patients are described in online supplemental table 1. Western blot analysis revealed that FL-GSDM-D was significantly decreased in both the cirrhotic and ACLF groups compared with the expression of healthy controls (figure 1B). However,

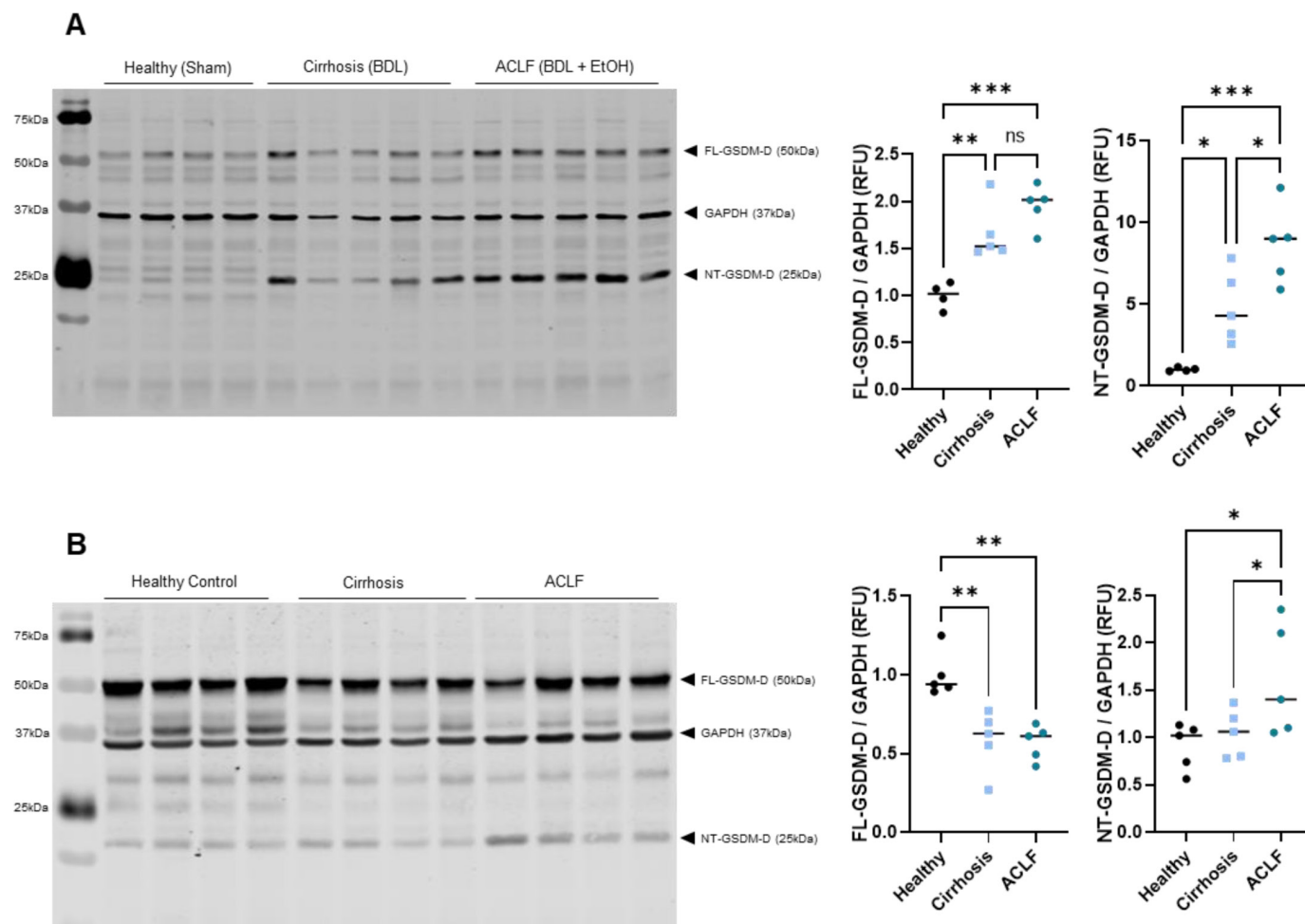


Figure 1 (A) Hepatic protein expression of GSDM-D in healthy, cirrhotic and ACLF mice. (B) Hepatic protein expression of GSDM-D in human specimens from healthy controls and patients with cirrhosis and ACLF. Western blot data were normalised to GAPDH levels. Data are expressed as mean \pm SD (n=4–5 per group). Statistical significance was determined using one-way analysis of variance: *p<0.05, **p<0.001, ***p<0.0001. ACLF, acute-on-chronic liver failure; BDL, bile duct ligation; EtOH, alcohol; FL-GSDM-D, full-length gasdermin D; GAPDH, glyceraldehyde-3-phosphate dehydrogenase; GSDM-D, gasdermin D; NT-GSDM-D, N-terminal gasdermin D; RFU, relative fluorescent unit.

patients with ACLF showed significantly higher levels of NT-GSDM-D compared with healthy controls or cirrhotic patients without ACLF, respectively (figure 1B).

GSDM-D-deficient mice undergoing ACLF exhibit reduced systemic and hepatic inflammation

Given the significant increase in NT-GSDM-D levels in ACLF livers and the key implication of pyroptosis in ACLF pathophysiology, we hypothesised that deficiency in GSDM-D may lead to an improvement in ACLF. For this, we established the ACLF model previously described in Ortega-Ribera *et al*⁷ in GSDM-D knockout (KO) or wild-type (WT) mice (figure 2A).

We first assessed how GSDM-D KO regulated inflammation (figure 2) and neutrophil infiltration (figure 3). In the circulation, GSDM-D KO mice exhibited less inflammation, as shown by a significant reduction in the percentage of pro-inflammatory Ly6C^{high} cells and a significant increase in the percentage of anti-inflammatory Ly6C^{low} cells (figure 2B). In the liver, GSDM-D-deficient mice exhibited decreased inflammation, as shown by a significant decrease

in the messenger RNA (mRNA) expression of monocyte chemoattractant protein 1 (*Mcp1*) and its receptor *Ccr2*, *Cd206*, *Cd32* and *Tnfa* (figure 2C), a significant decrease in the protein expression of IL-6 and a trend towards reducing MCP1 (figure 2D). CD68 immunohistochemistry showed no change in the levels of liver-infiltrated macrophages in the GSDM-D KO mice compared with WT mice (figure 2E).

Neutrophils were identified by flow cytometry as Ly6G-positive cells. Total neutrophil percentage or toll-like receptor 4 (TLR4)⁺-neutrophils or carcinoembryonic antigen-related cell adhesion molecule 8 (CEACAM8)⁺-neutrophils were not significantly different in WT or GSDM-D KO mice undergoing ACLF (figure 3A). In the liver, *Ly6g*, *Cxcl2* and the adhesion molecule *Icam1* were reduced in GSDM-D KO mice (figure 3B). At the protein level, GSDM-D KO mice exhibited decreased expression of neutrophil elastase (NE) and C-X-C motif chemokine ligand 1 (CXCL1) (figure 3C) and a trend towards decreasing Ly6G liver-infiltrating cells (figure 3D), further confirming the improvement in hepatic inflammation.

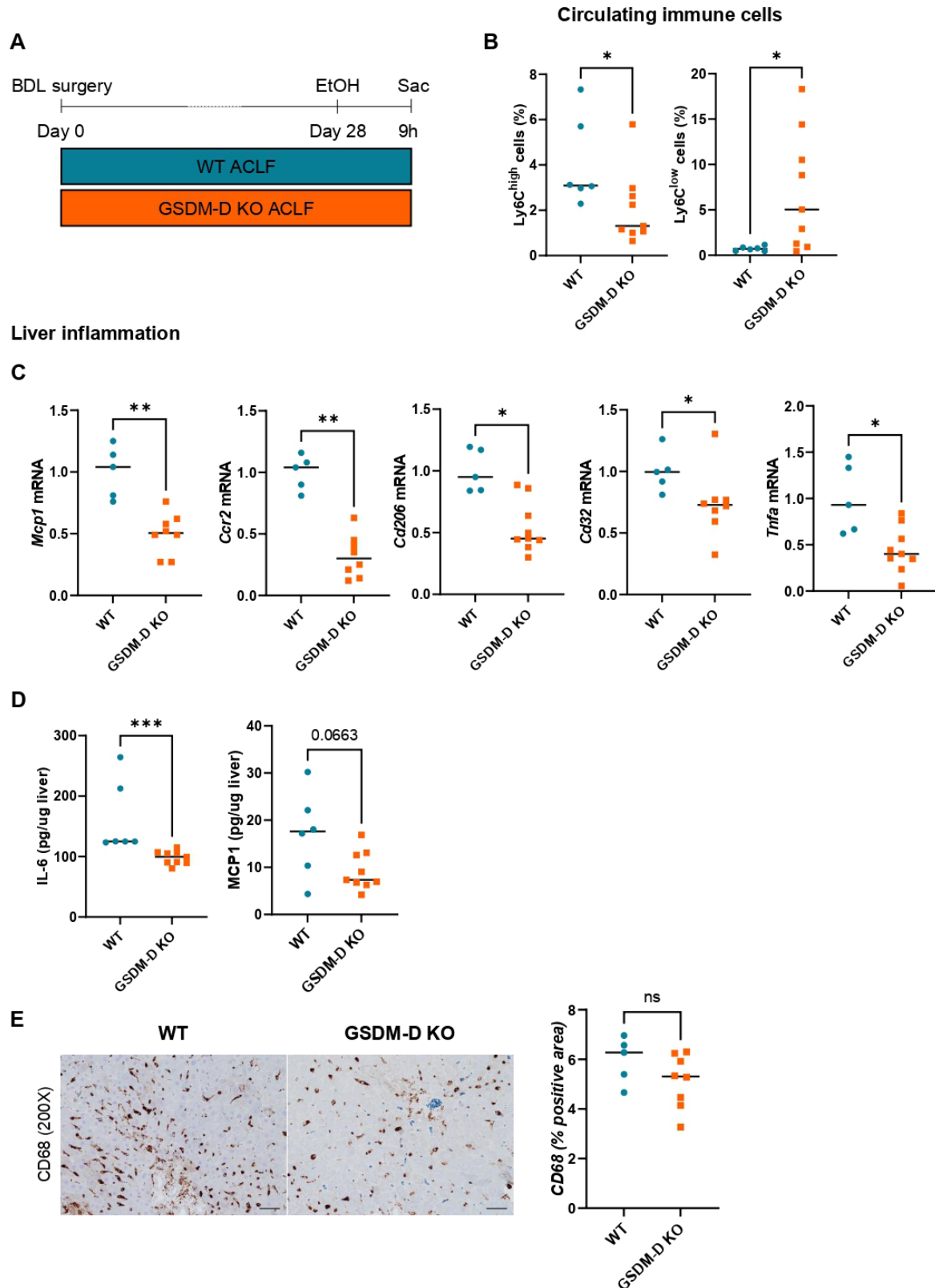
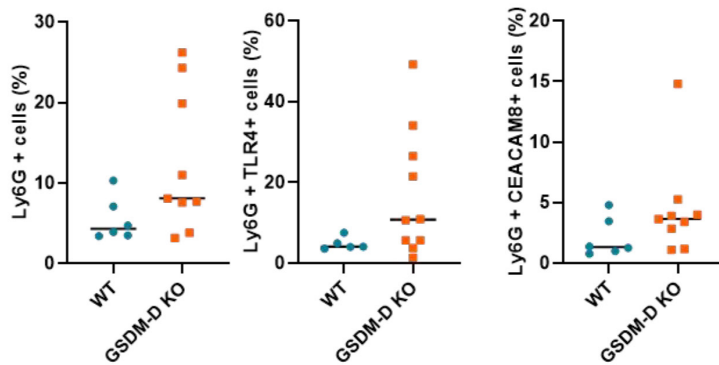
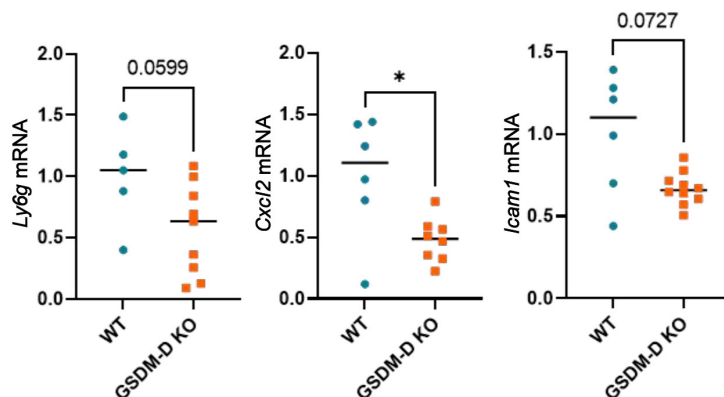


Figure 2 (A) Schematics of the murine model of ACLF in WT or GSDM-D KO mice. (B) Frequency of circulating monocytes (Ly6C^{high} and Ly6C^{low} cells) was analysed by flow cytometry. (C) Hepatic mRNA expression of inflammation markers including *Mcp1*, *Ccr2*, *Cd206*, *Cd32* and *Tnfr*. (D) Hepatic protein expression of inflammatory markers including IL-6 and MCP1 assessed by ELISA. (E) Representative images and quantification (% positive area) of CD68 immunohistochemistry in the liver. Scale bar for 200 \times : 50 μ m. Data are expressed as mean \pm SD (n=6–9 per group). Statistical significance was determined using two-tailed t-test: *p<0.05, **p<0.001, ***p<0.0001. ACLF, acute-on-chronic liver failure; BDL, bile duct ligation; EtOH, alcohol; GSDM-D, gasdermin D; IL-6, interleukin 6; KO, knockout; MCP1, monocyte chemoattractant protein 1; mRNA, messenger RNA; WT, wild-type.

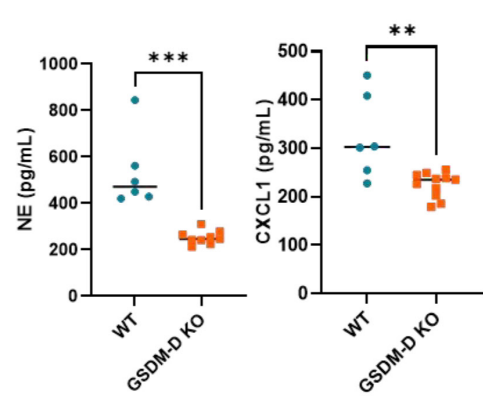
A Circulating neutrophils



B Neutrophil infiltration in the liver



C



D

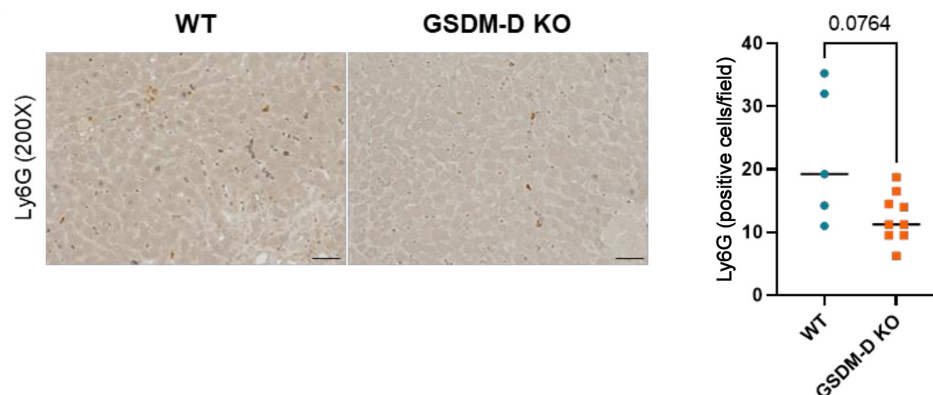


Figure 3 (A) Frequency of circulating neutrophils (Ly6G⁺ cells) and activation markers (TLR4 and CEACAM8) was analysed by flow cytometry. (B) Hepatic mRNA expression of inflammation markers including *Ly6g*, *Cxcl2* and *Icam1*. (C) Hepatic protein expression of neutrophil extracellular trap markers including NE and CXCL1 assessed by ELISA. (D) Representative images and quantification (number of positive cells per field) of Ly6G immunohistochemistry in the liver. Scale bar for 200×: 50 µm. Data are expressed as mean ± SD (n=6–9 per group). Statistical significance was determined using two-tailed t-test: *p<0.05, **p<0.001, ***p<0.0001. CEACAM8, carcinoembryonic antigen-related cell adhesion molecule 8; CXCL1, C-X-C motif chemokine ligand 1; GSDM-D, gasdermin D; KO, knockout; mRNA, messenger RNA; NE, neutrophil elastase; TLR4, toll-like receptor 4; WT, wild-type.

GSDM-D deficiency prevents cell death in the liver of ACLF mice

We next evaluated three main pathways of cell death, including apoptosis, pyroptosis and necroptosis, in the liver of GSDM-D or WT ACLF mice. GSDM-D KO mice showed reduced apoptosis, as evidenced by a significant reduction in the expression of cleaved CASP3 (figure 4A).

We also observed a significant increase in the expression of cl-CASP4 (figure 4B), without changes in the active form of CASP11 (figure 4C). Regarding pyroptosis, GSDM-D KO mice undergoing ACLF showed a trend towards a reduced expression of cleaved CASP1 (figure 4D) and IL-1β and a significant decrease in IL-18 (figure 4E) at the protein level, indicating inhibition of pyroptotic cell

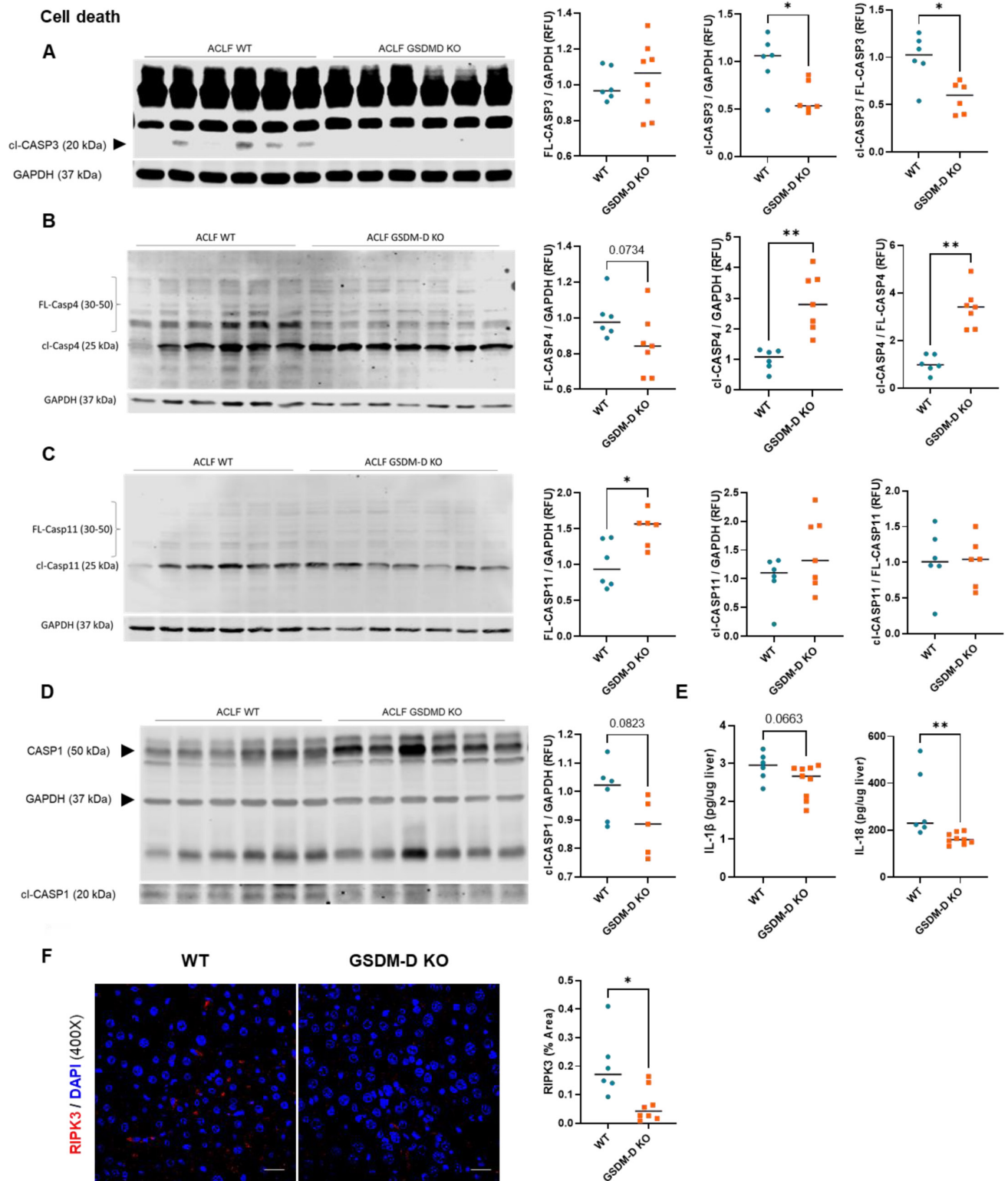


Figure 4 (A) Hepatic protein expression of CASP3 in WT or GSDMD-D KO mice with ACLF. (B) Hepatic protein expression of CASP4 in WT or GSDMD-D KO mice with ACLF. (C) Hepatic protein expression of CASP11 in WT or GSDMD-D KO mice with ACLF. (D) Hepatic protein expression of CASP1 in WT or GSDMD-D KO mice with ACLF. (E) IL-1 β (ELISA) and IL-18 (ELISA) levels in WT or GSDMD-D KO mice with ACLF. (F) Representative images and quantification of RIPK3 immunofluorescence in the liver were measured as a percentage of positive area per field. Scale bar for 400 \times : 20 μ m. Western blot data are represented as normalised to GAPDH levels and as the ratio between the cleaved form and the full-length form. Data are expressed as mean \pm SD (n=6–9 per group). Statistical significance was determined using two-tailed t-test: *p<0.05, **p<0.001. ACLF, acute-on-chronic liver failure; CASP, caspase; DAPI, 4',6-diamidino-2-phenylindole; FL, full length; GAPDH, glyceraldehyde-3-phosphate dehydrogenase; GSDMD-D, gasdermin D; IL, interleukin; KO, knockout; RFU, relative fluorescent unit; RIPK3, receptor-interacting serine/threonine kinase 3; WT, wild-type.

death. Moreover, receptor-interacting serine/threonine kinase 3 (RIPK3) expression was significantly reduced in GSDM-D-deficient ACLF mice, indicating a downregulation of necroptotic cell death (figure 4F).

GSDM-D deficiency attenuates liver fibrosis but impairs hepatocyte function in mice with ACLF

It has been demonstrated that the regenerative capacity of the liver is impaired during the progression of ACLF.^{15 16} This process is tightly regulated by inflammatory cues including cytokines and DAMPs from dying cells.^{16 17} Given the reduction in liver inflammation

and cell death in GSDM-D-deficient mice, we next assessed liver fibrosis and hepatocyte-related proliferative markers as hallmark pathways involved in liver regeneration.

Amelioration of liver fibrosis in GSDM-D KO mice undergoing ACLF was evidenced by a significant reduction in the liver mRNA expression of the fibrosis markers *Col1a1* and *Mmp12* and a trend towards decreasing *Acta2* levels (figure 5A). Moreover, attenuated fibrosis was confirmed by a significant reduction in the percentage of fibrotic areas in the liver on Sirius red staining (figure 5B).

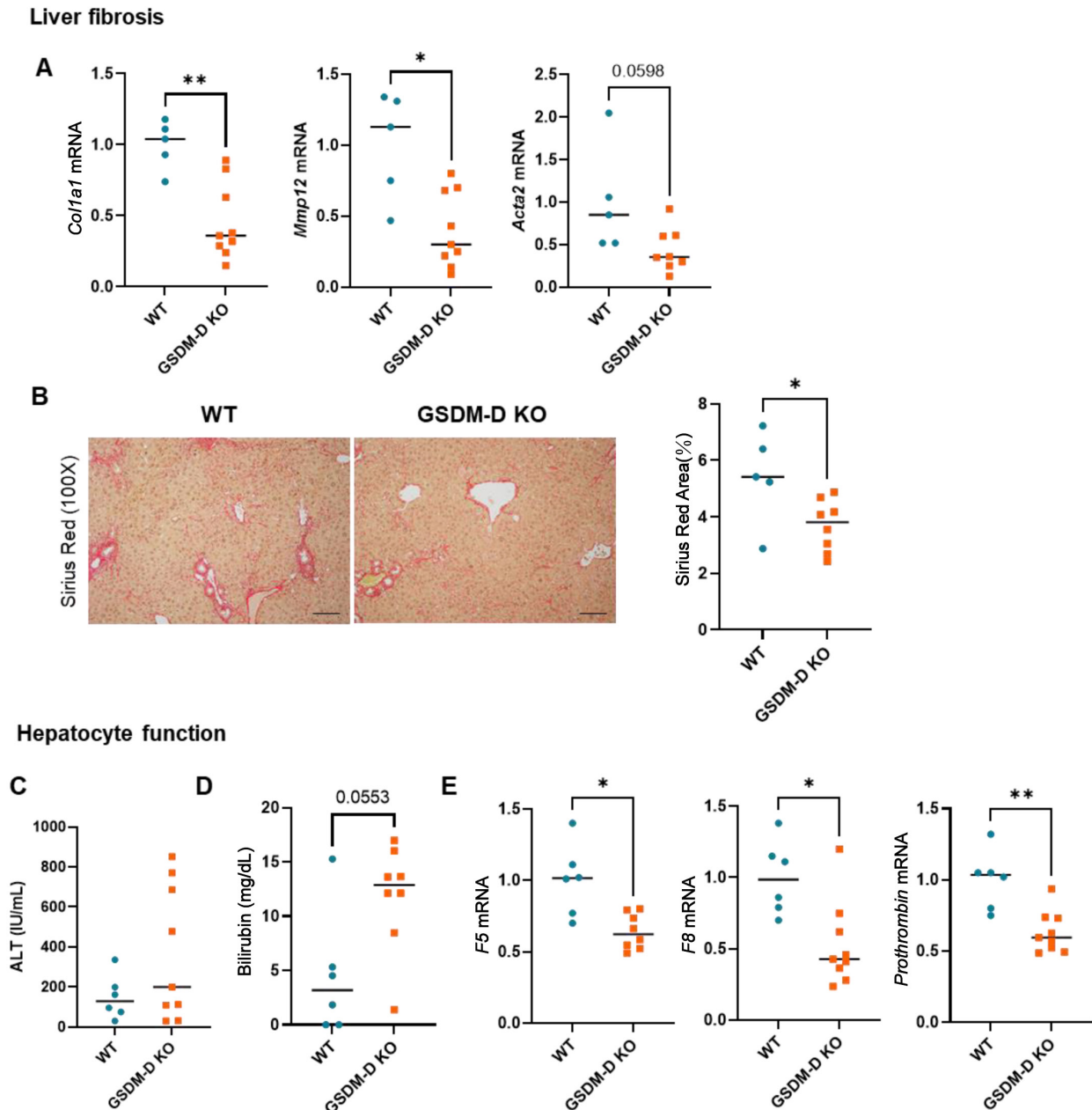


Figure 5 (A) Hepatic mRNA expression of fibrosis markers including *Col1a1*, *Mmp12* and *Acta2*. (B) Sirius red representative images and quantification in percentage area. Scale bar for 100x: 100 μ m. (C) ALT serum levels. (D) Bilirubin levels in serum. (E) Hepatic mRNA expression of coagulation markers including *F5*, *F8* and *prothrombin*. Data are expressed as mean \pm SD (n=6–9 per group). Statistical significance was determined using two-tailed t-test: *p<0.05, **p<0.001. ALT, alanine aminotransferase; GSDM-D, gasdermin D; KO, knockout; mRNA, messenger RNA; WT, wild-type.

Serum alanine aminotransferase (ALT) levels remained unchanged in both ACLF groups (figure 5C), while serum bilirubin levels trended towards an increase in GSDM-D-deficient mice in ACLF (figure 5D). Furthermore, we found a significant decrease in the hepatic mRNA expression of coagulation markers including *F5*, *F8* and *prothrombin* (figure 5E), indicating an impairment in hepatocyte function of GSDM-D KO on ACLF.

Deficiency in GSDM-D in ACLF mice induces senescence and dysregulates liver regeneration markers in mice with ACLF

Given the impairment in hepatocyte function in GSDM-D-deficient mice in ACLF, we further characterised hepatocyte function in the ACLF model. We found that GSDM-D KO induced an increase in the mRNA expression of senescence markers in the liver, including *Cdkn1a* and *Serpin1* (figure 6A). Interestingly, mRNA expression of stemness markers including *Nanog* and *Cd133* (figure 6B) and ductular reaction markers such as keratin (*Krt*) 7 and *Krt19* (figure 6C) was also increased in the liver of GSDM-D KO mice compared with WT. Increased expression of KRT7 in GSDM-D KO mice undergoing ACLF was validated by immunohistochemistry (IHC) in liver sections (figure 6D).

Regarding liver regeneration, we observed a significant reduction in the expression of the proliferation marker *Mki67* and the progenitor markers *Afp* and *Snai1* (figure 6E). No significant change was found in *Hgf* expression in response to GSDM-D deficiency in ACLF (figure 6E). Ki67 downregulation in the GSDM-D KO mice was validated at the protein level by immunohistochemistry (figure 6F). Overall, these data suggest that GSDM-D deficiency contributes to senescence of hepatocytes, ductular reaction and ineffective regenerative response in GSDM-D-deficient mice.

GSDM-D KO in alcohol-induced ACLF increases kidney damage

ACLF is defined as a multiorgan syndrome where the kidney and the brain (encephalopathy) are the most frequently affected systems outside of the liver.^{18 19} Given the impairment in hepatocyte function, we sought to investigate the potential function of GSDM-D deficiency in influencing kidney and brain pathophysiology. We first assessed renal histology and found that GSDM-D KO mice with ACLF showed histological damage, as indicated by a higher pathology score considering tubular dilation, interstitial hypercellularity, protein cast formation and neutrophil infiltration (figure 7A). Moreover, GSDM-D KO mice exhibited higher circulating levels of blood urea nitrogen (BUN) and a trend towards increasing kidney injury marker 1 (KIM-1) levels in the serum compared with WT mice with ACLF (figure 7B,C respectively). We also observed an increase in neutrophil infiltration in the kidney of GSDM-D KO mice undergoing ACLF, as shown by a significant increase in the mRNA renal expression of *Ly6g* and *Cxcl1* (figure 7D). Finally, we assessed landmark markers for cell death and senescence in kidney lysates.

Renal data showed an upregulation of genes related to necroptosis, including *Ripk3* and *Mlkl* (figure 7E), on GSDM-D deficiency. We also observed a significant increase in the expression of the senescence marker *Cdkn1a* but a reduction in *Serpin1* (figure 7E).

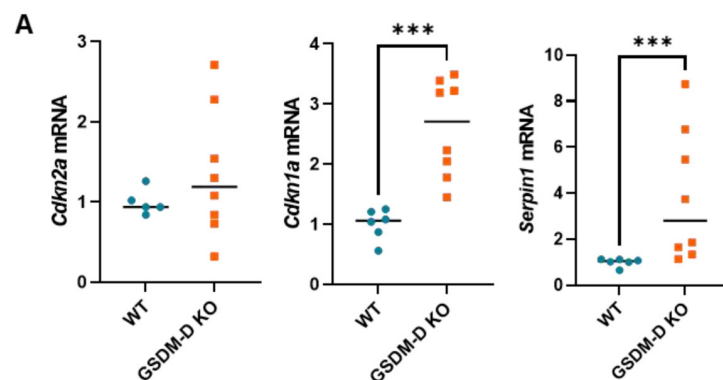
GSDM-D deficiency in ACLF exacerbates neuroinflammation, astrocytosis and apoptotic cell death in the cerebellum

In ACLF and liver failure, hepatic encephalopathy is an indicator of a poor clinical prognosis.^{18 20 21} The cerebellum area in the brain is highly susceptible to ammonia, as we have previously demonstrated in this ACLF model.⁷ We found that the neuroinflammation-related marker *Hmox1* was markedly higher in the cerebellum of GSDM-D-deficient ACLF mice compared with WT (figure 8A). This was accompanied by a trend towards an increase in the levels of *Il-1β* and *Cxcl2* (figure 8A). We next analysed landmark activation genes for the three main cell types in the cerebellum: microglia, astrocytes and neurons. No significant change was observed in the mRNA expression levels of genes related to microglia activation (*Aif1*) and homeostasis (*P2ry12* and *Gpr34*) (figure 8B); however, astrocyte activation was suggested by an increase in the expression of *Gfap* in GSDM-D KO mice, as well as an increasing trend in the astrocytic glutamate transporter *Eaat2* (figure 8C). In the neuronal compartment, we found significant changes in the expression of neuronal and synaptic markers including *Neun*, *Nefl*, *Syt1*, *Syp* and *Psd95* (figure 8D). Finally, we found a significant increase in the expression of the senescence marker *Cdkn1a*, as well as in the expression of *proCasp3*, *Fas* and *Tnfrsf10b*, and a downregulation of the antiapoptotic molecule *Bcl2* (figure 8E). Moreover, we found a significant decrease in the necroptosis markers *Ripk1* and *Mlkl* and in the pyroptotic markers *proCasp1*, *Gsdmd* and *Il-18* (figure 8E). These data indicate an increase in senescence and apoptosis pathways and a decrease in necroptosis and pyroptosis signalling in the cerebellum of GSDM-D-deficient mice on ACLF.

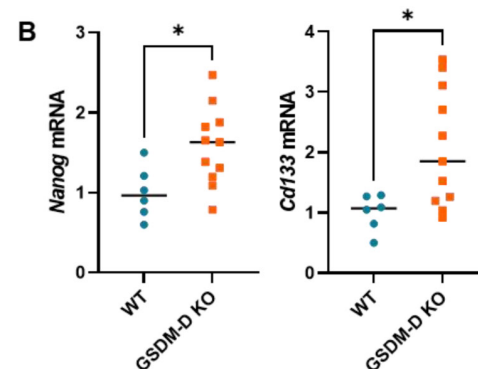
DISCUSSION

Pyroptosis is the process of inflammatory cell death aimed at defending the host against pathogen infection.²² GSDM-D is the central executor of pyroptosis, transducing the inflammatory signal from inflammasomes to membrane pore formation and facilitating pro-inflammatory cytokine release, for example, IL-1β/IL-18.^{8 9} Pyroptosis has been recently identified as a central pathway in the pathophysiology of ACLF^{6 10} and more recently in the specific context of alcohol-induced ACLF.^{7 23} In this manuscript, we evaluated the role of GSDM-D deficiency in a murine model of alcohol-induced ACLF and described its implications at the multiorgan level, including the liver, kidney and brain. Our study illustrates that active GSDM-D expression is increased in ACLF. Furthermore, a potential dual effect of pyroptosis inhibition by using GSDM-D KO mice in

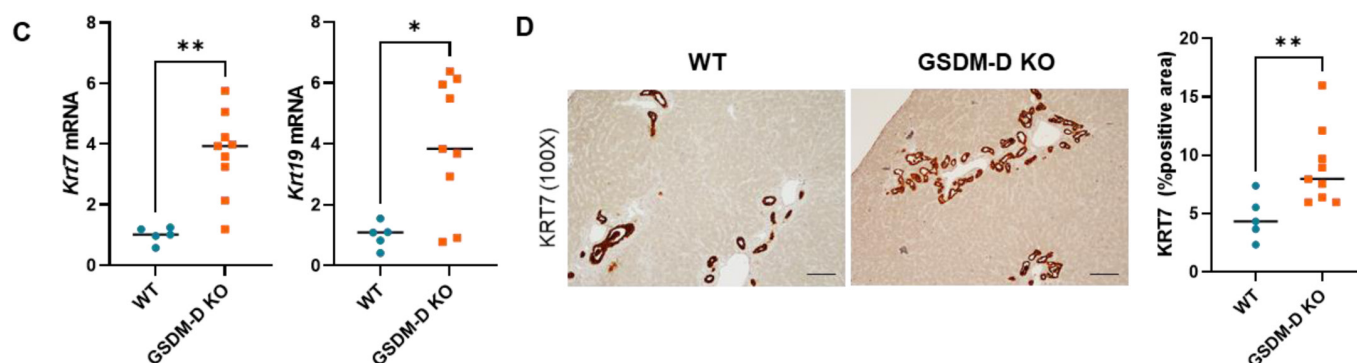
Senescence-associated markers



Stem-like features



Ductular reaction / Cholangiocyte



Liver proliferation

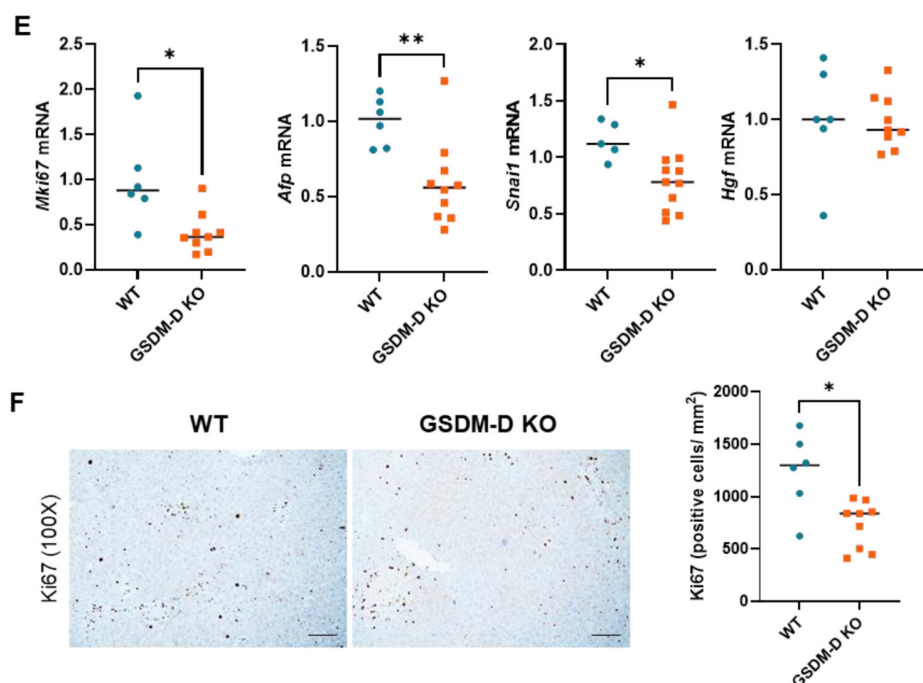


Figure 6 (A) Hepatic mRNA expression of senescence markers including *Cdkn2a*, *Cdkn1a* and *Serpin1*. (B) Hepatic mRNA expression of stem-like markers including *Nanog* and *Cd133*. (C) Hepatic mRNA expression of ductular reaction/cholangiocyte markers including *Krt7* and *Krt19*. (D) Representative images and quantification (percentage of positive area) of KRT7 immunohistochemistry in the liver. (E) Hepatic mRNA expression of liver regeneration markers including *Mki67*, *Afp*, *Snai1* and *Hgf*. (F) Representative images and quantification (number of positive cells per field) of Ki67 immunohistochemistry in the liver. Scale bar for 100×: 100µm. Data are expressed as mean±SD (n=6–9 per group). Statistical significance was determined using two-tailed t-test: *p<0.05, **p<0.001, ***p<0.0001. GSDM-D, gasdermin D; KO, knockout; Krt, keratin; mRNA, messenger RNA; WT, wild-type.

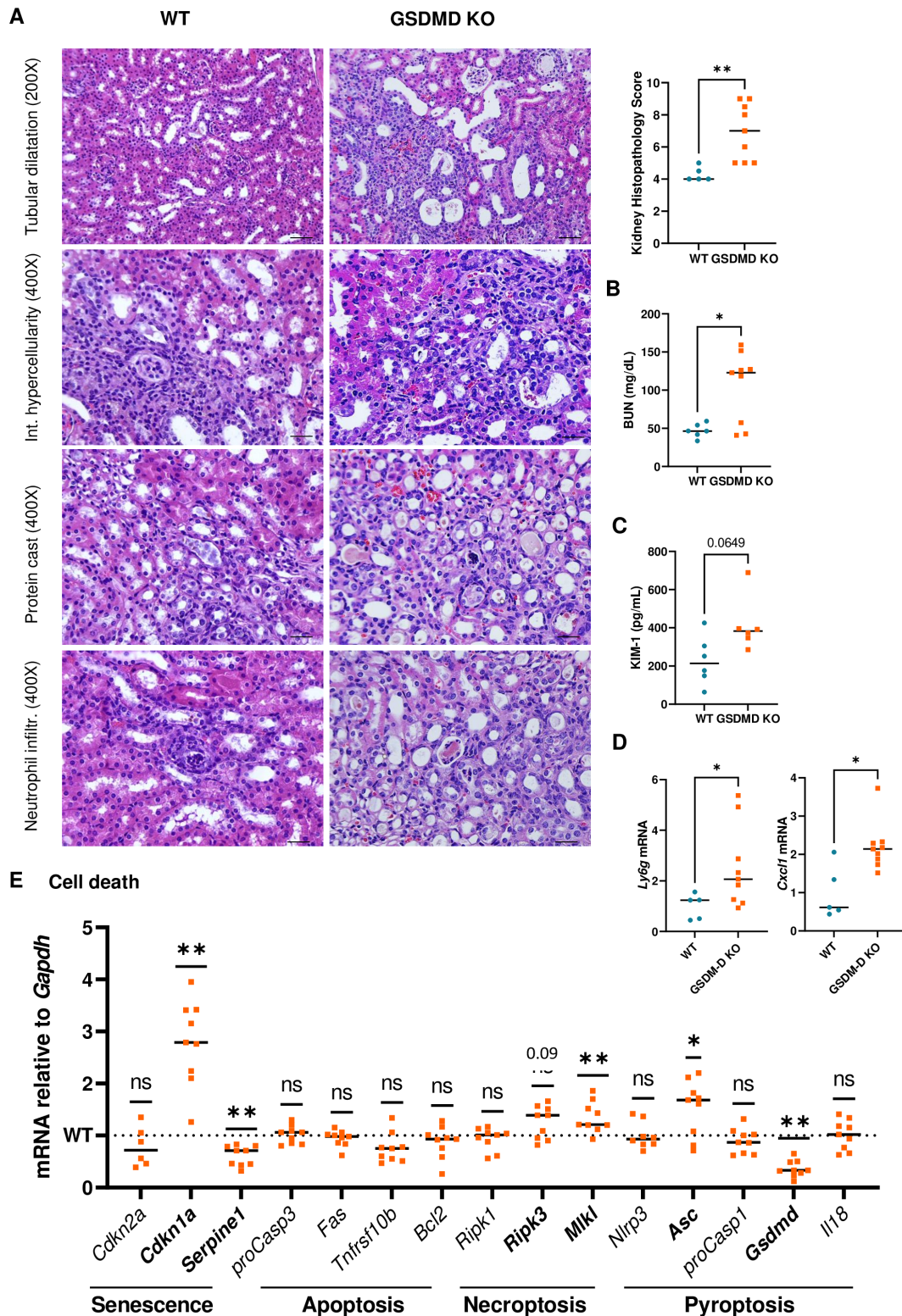


Figure 7 (A) Kidney histopathological score assessing tubular dilatation, interstitial hypercellularity, cortical and medullary tubular casts and neutrophil infiltration shown in the representative images from H&E staining in kidney sections (20× and 40× magnification). (B) BUN serum levels. (C) KIM-1 expression in the serum was assessed by ELISA. (D) Renal mRNA expression of neutrophil infiltration markers including *Ly6g* and *Cxcl1*. (E) Renal mRNA expression of senescence and cell death markers including *Cdkn2a*, *Cdkn1a*, *Serpine1*, *proCasp3*, *Fas*, *Tnfrsf10b*, *Bcl2*, *Ripk1*, *Ripk3*, *Mkl1*, *Nlrp3*, *Asc*, *proCasp1*, *Gsdmd* and *Il18*. qPCR levels are normalised to WT ACLF group, and the genes that significantly change are highlighted in bold. Scale bar for 200×: 50 µm; for 400×: 20 µm. Data are expressed as mean±SD (n=6–9 per group). Statistical significance was determined using two-tailed t-test: *p<0.05, **p<0.005. ACLF, acute-on-chronic liver failure; BUN, blood urea nitrogen; Cxcl1, C-X-C motif chemokine ligand 1; GAPDH, glyceraldehyde-3-phosphate dehydrogenase; GSDMD-D, gasdermin D; KIM-1, kidney injury marker 1; KO, knockout; mRNA, messenger RNA; qPCR, quantitative PCR; WT-wild-type.

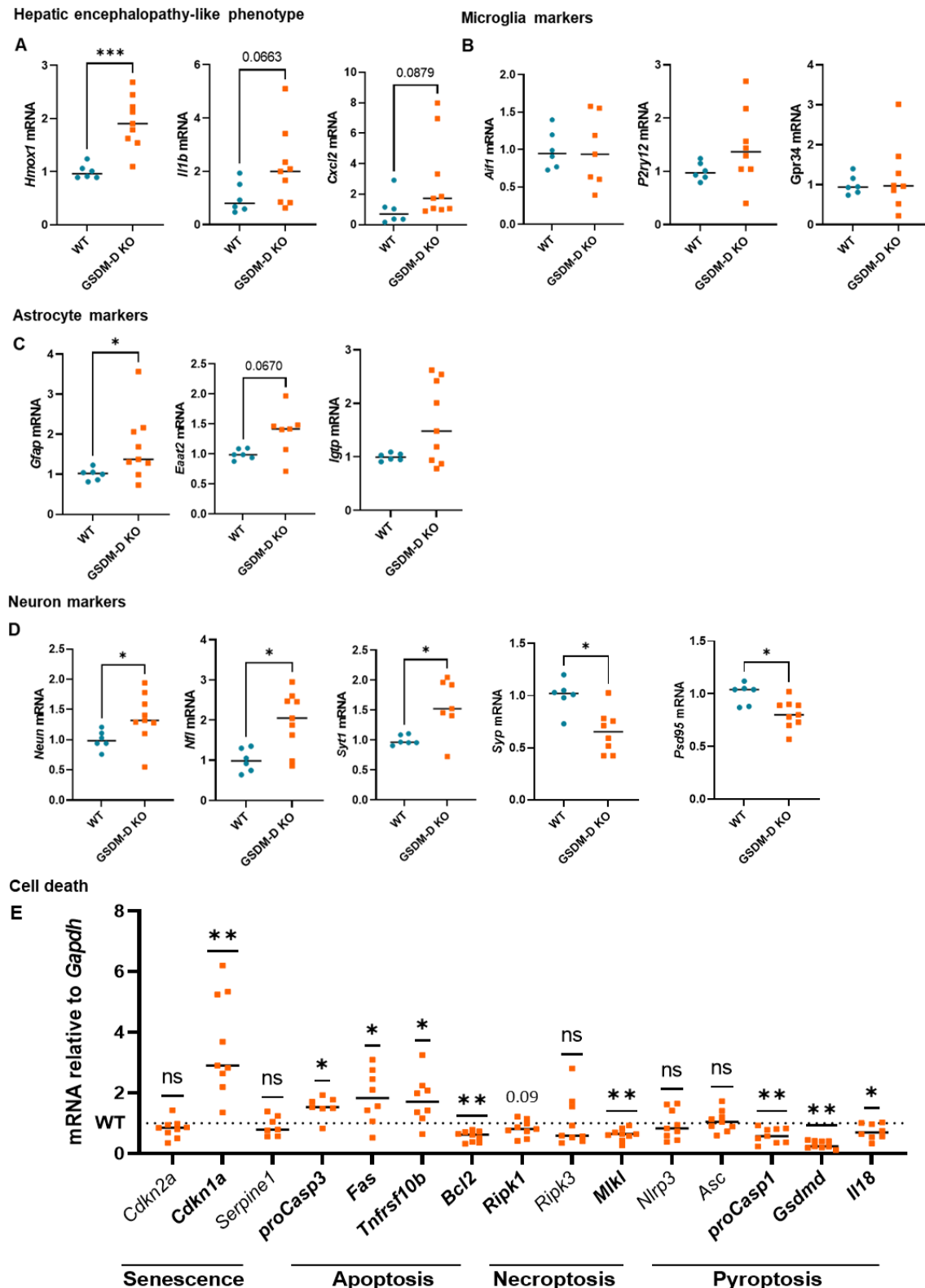


Figure 8 (A) Cerebellum mRNA expression of encephalopathy-related markers including *Hmxo1*, *Il-1b* and *Cxcl2*. (B) Cerebellum mRNA expression of microglia activation and homeostatic markers including *Aif1*, *P2ry12* and *Gpr34*. (C) Cerebellum mRNA expression of astrocyte activation markers including *Gfap*, *Eaat2* and *Igtp*. (D) Cerebellum mRNA expression of neuronal markers including *Neun*, *Nefl*, *Syp*, *Psd95* and *Syt1*. (E) Cerebellum mRNA expression of senescence and cell death markers including *Cdkn2a*, *Cdkn1a*, *Serpin1*, *proCasp3*, *Fas*, *Tnfrsf10b*, *Bcl2*, *Ripk1*, *Ripk3*, *Mki1*, *Nlrp3*, *Asc*, *proCasp1*, *Gsdmd* and *Il-18*. qPCR levels are normalised to the WT ACLF group, and the genes that significantly change are highlighted in bold. Data are expressed as mean±SD (n=6–9 per group). Statistical significance was determined using two-tailed t-test: *p<0.05, **p<0.005, ***p<0.0005. ACLF, acute-on-chronic liver failure; GAPDH, glyceraldehyde-3-phosphate dehydrogenase; GSDM-D, gasdermin D; KO, knockout; mRNA, messenger RNA; qPCR, quantitative PCR; WT, wild-type.

ACLF was identified, with a protective effect on the liver and detrimental effects on extrahepatic organs, including the kidney and brain.

The executor role of gasdermins in pyroptosis is well established.^{9–24} Recent studies identified additional homeostatic roles for gasdermins, such as mediators of organelle integrity and function, plasma membrane repair through ion gradients and sensors/responders to cellular stress.²⁵ In the context of liver injury, increased levels of GSDM-D and pyroptosis activation have been established in a wide variety of liver syndromes, including partial hepatectomy (PH),²⁶ metabolic dysfunction-associated steatohepatitis,²⁷ alcohol-associated hepatitis,²⁸ hepatitis B infection²⁹ and cholestatic fibrosis.¹² Here, we show that GSDM-D expression is also increased in a preclinical model of ACLF and in liver specimens from patients with ACLF, highlighting GSDM-D as a plausible target to ameliorate liver injury.

In order to examine whether GSDM-D deletion could ameliorate ACLF pathophysiology, we induced ACLF in WT or GSDM-D-deficient mice as recently described.⁷ GSDM-D deficiency in mice undergoing alcohol-induced ACLF was protective in the liver, as shown by a reduction in the expression of pro-inflammatory mediators, neutrophil infiltration, cell death and fibrosis. This protective effect of GSDM-D deficiency was in contrast to changes in hepatocytes that appeared to be arrested in the senescent state, as indicated by their increased expression of senescence markers (*Cdkn2a* and *Serpin1*), decreased regeneration and increased expression of stem-like and cholangiocyte markers. Deficiency in GSDM-D has been shown to improve liver damage, liver regeneration and pyroptosis (serum levels of IL-18 and IL-1 β) in a preclinical model of 48 hours and 72 hours of 70% PH.²⁶ Overexpression of mature GSDM-D in hepatocytes leads to increased hepatocyte death and neutrophil infiltration in a combined model of high cholesterol, saturated fat and alcohol model of alcohol-associated hepatitis.²⁸ Moreover, KO of GSDM-D improved liver damage in a model of polymicrobial sepsis by downregulating NET formation.³⁰ On the other hand, GSDM-D deletion has also been reported as detrimental in different models of liver injury. Mice with GSDM-D deficiency undergoing haemorrhagic shock with resuscitation or acetaminophen overdose showed increased liver damage (elevated ALT and extended death areas) at 6 hours compared with WT mice.³¹ This suggests that the protective effects of GSDM-D deletion are probably injury-specific and severity-specific. The contribution or absence of reactive oxygen species (ROS) might be an additional mechanism regulating this effect, with the absence of GSDM-D making hepatocytes more susceptible to ROS-mediated damage.³¹

ACLF is often associated with multiorgan dysfunction or failure, with the kidney and the brain being the most commonly impaired extrahepatic organs.³² We previously demonstrated that our alcohol-induced ACLF model involves kidney dysfunction and hepatic

encephalopathy-like damage in the brain.⁷ Thus, we assessed the implication of GSDM-D deficiency in these organs.

In the kidney, GSDM-D deficiency in ACLF triggered impaired kidney function and worsened the histopathological score compared with WT ACLF mice. Moreover, we also observed an upregulation of necroptosis-related genes, including *Ripk3* and *Mkl1*. Similar to our findings, Tonnus and colleagues reported that GSDM-D-deficient mice showed hypersensitivity to injury assessed as tubular damage and impaired function (increased serum creatinine and BUN) in acute kidney injury murine models induced by ischaemia/reperfusion (I/R) injury, calcium oxalate or cisplatin.³³ Interestingly, codeletion of the necroptosis executor *Mkl1* and GSDM-D reversed the hypersensitivity phenotype in the I/R injury model,³³ validating a major role of necroptosis in pyroptosis inhibition in the kidney.

In the brain, ACLF development in GSDM-D-deficient mice increased the expression of hepatic encephalopathy-related markers including *Hmox1*, *Il-1b* and *Cdkn1a*. Despite no changes in the expression of microglia activation and homeostasis markers, we identified astrocyte activation and changes in neuronal markers, suggesting synaptic alterations together with an increase in apoptosis-related cell death markers in the cerebellum. However, more detailed studies would need to be performed to unravel the effect of GSDM-D deletion on neuronal activity and survival. Other studies reported GSDM-D deficiency to reduce brain damage by ameliorating leucocyte recruitment and preventing pro-inflammatory cytokine release in models of ischaemic stroke or cerebral ischaemia.^{34–35} Another study showed that GSDM-D deletion exerted neuroprotective effects on motor dysfunction and neuropathological alterations (loss of synaptic proteins, microglia activation, astrogliosis) after traumatic brain injury.³⁶ We understand that these studies address the organ-specific role of GSDM-D manipulation in the brain itself as opposed to secondary damage after liver dysfunction. We speculate that the potential protective effect of GSDM-D deletion in the brain is overcome by the damage induced by liver and kidney dysfunction in the context of ACLF. Moreover, the contributing role of GSDM-D might be different in acute injuries like I/R injury or traumatic brain injury compared with chronic injuries such as ACLF, where further studies are needed.

Finally, our study highlights a potential dual (beneficial or detrimental) role of GSDM-D in liver and organ injury that is likely cell type-specific and organ-specific. In the liver, we found protection from inflammation and fibrosis that could be related to GSDM-D in immune cells and/or myofibroblasts, while in hepatocytes GSDM-D deficiency appears to dysregulate important cell renewal functions. Increased kidney injury and neuroinflammation in GSDM-D-deficient mice with ACLF may suggest a protective role of GSDM-D in the injury of these organs, which is consistent with previous reports in the kidney and liver. In fact, we observed that necroptosis or apoptosis is

increased in the kidney and brain on GSDM-D deletion, probably influencing organ function in the absence of GSDM-D expression.

We acknowledge two limitations in this study. First, the usage of constitutive GSDM-D KO mice entails that the observed phenotype might be partly mediated by the early prevention of chronic liver disease development. Second, both WT and GSDM-D mice were in the C57BL/6N strain genetic background, which is known to be more resistant to alcohol injury, potentially underestimating the effect of alcohol-induced acute damage. Further studies dissecting the cell-specific role of GSDM-D deletion will be key to understanding the implication of GSDM-D-mediated cell death and interorgan crosstalk during ACLF.

In summary, this study highlights the key role of GSDM-D in ACLF. Deficiency of GSDM-D in a murine model of alcohol-induced ACLF ameliorated inflammation, neutrophil activation and cell death in the liver together with decreased regenerative response including fibrosis. Dysfunctional hepatocytes, probably inclined to a senescence state, lead to hepatocyte dysfunction, further impacting extrahepatic (kidney and brain) organ function and cell death pathways. Overall, our observations suggest a protective role for GSDM-D in the liver, but exacerbated extrahepatic damage in ACLF.

Author affiliations

¹Department of Medicine, Division of Gastroenterology, Beth Israel Deaconess Medical Center, Harvard Medical School, Boston, Massachusetts, USA

²Department of Medicine, Division of Nephrology, Beth Israel Deaconess Medical Center, Harvard Medical School, Boston, Massachusetts, USA

³Broad Institute, Cambridge, Massachusetts, USA

Acknowledgements The authors would like to acknowledge Histology Core at the BIDMC for their help in tissue sectioning and staining. The figures were created with Biorender.

Contributors MO-R, YZ and GS planned and designed the experiments and analysed and interpreted the data. MO-R and YZ conducted the experiments. MO-R and GS wrote the manuscript. MO-R, YZ, VB, RSJ, ZZ, PTN and AD conducted the experiments and analysed and discussed the data. All authors critically reviewed the manuscript. GS obtained funding and is the guarantor.

Funding This study was supported by NIH grants R01 AG072899, R01 AA017729 and R01 AA011576 (to GS).

Competing interests GS reports being a paid consultant for Evive Bio, Merck, Durect Corporation, Terra Firma, Pandion Therapeutics, Satellite Bio, LabCorp, Cyta Therapeutics, Pfizer, Takeda, Intercept, Surrozen, Resolution and Novo Nordisk. She holds stock options in Glympse and Zomagen Biosciences/Ventyx Biosciences and receives royalties from Springer Nature Group and UpToDate. GS is an Associate Editor of the *eGastroenterology*.

Patient and public involvement Patients and/or the public were not involved in the design, or conduct, or reporting, or dissemination plans of this research.

Patient consent for publication Not required.

Ethics approval Mouse experiments conducted in this study were approved by the BIDMC Institutional Animal Care and Use Committee (protocols 010-2019 and 030-2022).

Provenance and peer review Not commissioned; externally peer reviewed.

Data availability statement All data relevant to the study are included in the article or uploaded as supplementary information.

Supplemental material This content has been supplied by the author(s). It has not been vetted by BMJ Publishing Group Limited (BMJ) and may not have been peer-reviewed. Any opinions or recommendations discussed are solely those

of the author(s) and are not endorsed by BMJ. BMJ disclaims all liability and responsibility arising from any reliance placed on the content. Where the content includes any translated material, BMJ does not warrant the accuracy and reliability of the translations (including but not limited to local regulations, clinical guidelines, terminology, drug names and drug dosages), and is not responsible for any error and/or omissions arising from translation and adaptation or otherwise.

Open access This is an open access article distributed in accordance with the Creative Commons Attribution Non Commercial (CC BY-NC 4.0) license, which permits others to distribute, remix, adapt, build upon this work non-commercially, and license their derivative works on different terms, provided the original work is properly cited, appropriate credit is given, any changes made indicated, and the use is non-commercial. See: <http://creativecommons.org/licenses/by-nc/4.0/>.

ORCID iD

Gyongyi Szabo <http://orcid.org/0000-0003-0836-2527>

REFERENCES

- Karvellas CJ, Bajaj JS, Kamath PS, *et al.* AASLD Practice Guidance on Acute-on-chronic liver failure and the management of critically ill patients with cirrhosis. *Hepatology* 2024;79:1463–502.
- Bajaj JS, O'Leary JG, Lai JC, *et al.* Acute-on-Chronic Liver Failure Clinical Guidelines. *Am J Gastroenterol* 2022;117:225–52.
- Moreau R, Tonon M, Krag A, *et al.* EASL Clinical Practice Guidelines on acute-on-chronic liver failure. *J Hepatol* 2023;79:461–91.
- Moreau R. The Pathogenesis of ACLF: The Inflammatory Response and Immune Function. *Semin Liver Dis* 2016;36:133–40.
- Martin-Mateos R, Alvarez-Mon M, Albillos A. Dysfunctional Immune Response in Acute-on-Chronic Liver Failure: It Takes Two to Tango. *Front Immunol* 2019;10:973.
- Ye Q, Wang H, Chen Y, *et al.* PANoptosis-like death in acute-on-chronic liver failure injury. *Sci Rep* 2024;14:392.
- Ortega-Ribera M, Zhuang Y, Babuta M, *et al.* A Novel Multi-organ Male Model of Alcohol-induced Acute-on-chronic Liver Failure Reveals NET-mediated Hepatocellular Death, Which is Prevented by RIPK3 Inhibition. *Cell Mol Gastroenterol Hepatol* 2024;19:101446.
- Yu P, Zhang X, Liu N, *et al.* Pyroptosis: mechanisms and diseases. *Signal Transduct Target Ther* 2021;6:128.
- He W, Wan H, Hu L, *et al.* Gasdermin D is an executor of pyroptosis and required for interleukin-1 β secretion. *Cell Res* 2015;25:1285–98.
- Zhao Q, Chen D-P, Chen H-D, *et al.* NK-cell-elicited gasdermin-D-dependent hepatocyte pyroptosis induces neutrophil extracellular traps that facilitate HBV-related acute-on-chronic liver failure. *Hepatology* 2025;81:917–31.
- Kayagaki N, Stowe IB, Lee BL, *et al.* Caspase-11 cleaves gasdermin D for non-canonical inflammasome signalling. *Nature New Biol* 2015;526:666–71.
- Zhuang Y, Ortega-Ribera M, Thevkar Nagesh P, *et al.* Bile acid-induced IRF3 phosphorylation mediates cell death, inflammatory responses, and fibrosis in cholestasis-induced liver and kidney injury via regulation of ZBP1. *Hepatology* 2024;79:752–67.
- Uppal H, Saini SPS, Moschetta A, *et al.* Activation of LXRs prevents bile acid toxicity and cholestasis in female mice. *Hepatology* 2007;45:422–32.
- Bertola A, Mathews S, Ki SH, *et al.* Mouse model of chronic and binge ethanol feeding (the NIAAA model). *Nat Protoc* 2013;8:627–37.
- Xiang X, Feng D, Hwang S, *et al.* Interleukin-22 ameliorates acute-on-chronic liver failure by reprogramming impaired regeneration pathways in mice. *J Hepatol* 2020;72:736–45.
- Lange CM, Al-Juboori K, Rawitzer J, *et al.* Cirrhosis-Based Acute-on-Chronic Liver Failure Is Marked by Inflammation and Impaired Liver Regeneration Despite Stat3 Activation. *Gastro Hep Adv* 2022;1:520–30.
- Qiang R, Liu X-Z, Xu J-C. The Immune Pathogenesis of Acute-On-Chronic Liver Failure and the Danger Hypothesis. *Front Immunol* 2022;13:935160.
- Badal BD, Bajaj JS. Hepatic Encephalopathy in Acute-on-Chronic Liver Failure. *Clin Liver Dis* 2023;27:691–702.
- Br VK, Sarin SK. Acute-on-chronic liver failure: Terminology, mechanisms and management. *Clin Mol Hepatol* 2023;29:670–89.
- Verma N, Dhiman RK, Choudhury A, *et al.* Dynamic assessments of hepatic encephalopathy and ammonia levels predict mortality in acute-on-chronic liver failure. *Hepatol Int* 2021;15:970–82.
- Wang L, Zhu S, Liu Y, *et al.* Prognostic value of decline in model for end-stage liver disease score and hepatic encephalopathy in hepatitis B-related acute-on-chronic liver failure patients treated with plasma exchange. *Scand J Gastroenterol* 2022;57:1089–96.

- 22 Wu Y, Zhang J, Yu S, *et al.* Cell pyroptosis in health and inflammatory diseases. *Cell Death Discov* 2022;8:191.
- 23 Taru V, Szabo G, Mehal W, *et al.* Inflammasomes in chronic liver disease: Hepatic injury, fibrosis progression and systemic inflammation. *J Hepatol* 2024;81:895–910.
- 24 Tsuchiya K, Hosojima S, Hara H, *et al.* Gasdermin D mediates the maturation and release of IL-1 α downstream of inflammasomes. *Cell Rep* 2021;34:108887.
- 25 Weindel CG, Ellzey LM, Martinez EL, *et al.* Gasdermins gone wild: new roles for GSDMs in regulating cellular homeostasis. *Trends Cell Biol* 2023;33:773–87.
- 26 Lv X, Chen J, He J, *et al.* Gasdermin D-mediated pyroptosis suppresses liver regeneration after 70% partial hepatectomy. *Hepatol Commun* 2022;6:2340–53.
- 27 Xu B, Jiang M, Chu Y, *et al.* Gasdermin D plays a key role as a pyroptosis executor of non-alcoholic steatohepatitis in humans and mice. *J Hepatol* 2018;68:773–82.
- 28 Khanova E, Wu R, Wang W, *et al.* Pyroptosis by caspase11/4-gasdermin-D pathway in alcoholic hepatitis in mice and patients. *Hepatology* 2018;67:1737–53.
- 29 Xie W, Ding J, Xie X, *et al.* Hepatitis B virus X protein promotes liver cell pyroptosis under oxidative stress through NLRP3 inflammasome activation. *Inflamm Res* 2020;69:683–96.
- 30 Silva CMS, Wanderley CWS, Veras FP, *et al.* Gasdermin D inhibition prevents multiple organ dysfunction during sepsis by blocking NET formation. *Blood* 2021;138:2702–13.
- 31 Yang C, Sun P, Deng M, *et al.* Gasdermin D protects against noninfectious liver injury by regulating apoptosis and necroptosis. *Cell Death Dis* 2019;10:481.
- 32 Arroyo V, Moreau R, Kamath PS, *et al.* Acute-on-chronic liver failure in cirrhosis. *Nat Rev Dis Primers* 2016;2:16041.
- 33 Tonnus W, Maremonti F, Belavgeni A, *et al.* Gasdermin D-deficient mice are hypersensitive to acute kidney injury. *Cell Death Dis* 2022;13:792.
- 34 Hu R, Liang J, Ding L, *et al.* Gasdermin D inhibition ameliorates neutrophil mediated brain damage in acute ischemic stroke. *Cell Death Discov* 2023;9:50.
- 35 Wang K, Sun Z, Ru J, *et al.* Ablation of GSDMD Improves Outcome of Ischemic Stroke Through Blocking Canonical and Non-canonical Inflammasomes Dependent Pyroptosis in Microglia. *Front Neurol* 2020;11:577927.
- 36 Du H, Li C-H, Gao R-B, *et al.* Ablation of GSDMD Attenuates Neurological Deficits and Neuropathological Alterations After Traumatic Brain Injury. *Front Cell Neurosci* 2022;16:915969.